Video Article

Automatic Detection of Highly Organized Theta Oscillations in the Murine EEG

Ralf Müller[1], Anna Papazoglou[2], Julien Soos[2], Andreas Lundt[2], Carola Wormuth[2], Christina Henseler[2], Dan Ehninger[3], Karl Broich[4], Marco Weiergräber[2]

[1]Department of Psychiatry and Psychotherapy, University of Cologne

[2]Department of Neuropsychopharmacology, Federal Institute for Drugs and Medical Devices

[3]Molecular and Cellular Cognition Lab, German Center for Neurodegenerative Diseases

[4]Federal Institute for Drugs and Medical Devices

Correspondence to: Marco Weiergräber at Marco.Weiergraeber@bfarm.de

URL: https://www.jove.com/video/55089
DOI: doi:10.3791/55089

Keywords: Behavior, Issue 121, electroencephalogram, hippocampus, mouse, oscillation, radiotelemetry, theta, time-frequency analysis

Date Published: 3/10/2017

Citation: Müller, R., Papazoglou, A., Soos, J., Lundt, A., Wormuth, C., Henseler, C., Ehninger, D., Broich, K., Weiergräber, M. Automatic Detection of Highly Organized Theta Oscillations in the Murine EEG. *J. Vis. Exp.* (121), e55089, doi:10.3791/55089 (2017).

Abstract

Theta activity is generated in the septohippocampal system and can be recorded using deep intrahippocampal electrodes and implantable electroencephalography (EEG) radiotelemetry or tether system approaches. Pharmacologically, hippocampal theta is heterogeneous (see dualistic theory) and can be differentiated into type I and type II theta. These individual EEG subtypes are related to specific cognitive and behavioral states, such as arousal, exploration, learning and memory, higher integrative functions, etc. In neurodegenerative diseases such as Alzheimer's, structural and functional alterations of the septohippocampal system can result in impaired theta activity/oscillations. A standard quantitative analysis of the hippocampal EEG includes a Fast-Fourier-Transformation (FFT)-based frequency analysis. However, this procedure does not provide details about theta activity in general and highly-organized theta oscillations in particular. In order to obtain detailed information on highly-organized theta oscillations in the hippocampus, we have developed a new analytical approach. This approach allows for time- and cost-effective quantification of the duration of highly-organized theta oscillations and their frequency characteristics.

Video Link

The video component of this article can be found at https://www.jove.com/video/55089/

Introduction

Theta activity in the brain is related to different cognitive and functional states, including arousal, attention, voluntary movement, exploratory behavior, attention behavior, learning and memory, somatosensory integration, and rapid eye movement (REM) sleep[1,2]. Principally, theta activity as a rhythmic entity can be generated in various cerebral regions and is highly organized and synchronized as theta oscillations. Below, we will focus on the analysis and quantification of theta activity/oscillations that are generated within the septohippocampal system[3,4]. Within the septum, GABAergic, glutamatergic, and cholinergic neurons project to the hippocampus and contribute to the initiation and maintenance of theta oscillatory behavior. There is an ongoing discussion on whether hippocampal theta oscillations are initiated in the septum, *i.e.,* the septal pacemaker-hippocampal follower model, (extrahippocampal theory) or intrinsically within the hippocampus (intrahippocampal theory)[5,6,7].

Regardless of their origin, hippocampal theta oscillations have been in the focus of interest for years, particularly in transgenic mouse models. These models allow for the implantation of deep EEG electrodes and for the recording of hippocampal theta oscillations under specific cognitive and behavioral tasks[8]. Hippocampal theta oscillations are heterogenous in nature. Based on the so-called dualistic theory of theta oscillations, one can differentiate between atropine-sensitive type II theta and atropine-insensitive type I theta[9,10,11]. The latter can typically be induced by muscarinic M_1/M_3 receptor agonists, *e.g.,* arecoline, pilocarpine, and urethane. However, urethane is a multi-target drug that, besides muscarinic activation, also exerts complex effects on other ion channel entities. For type II theta, the muscarinic pathway includes the activation of M_1/M_3 and a subsequent $G_{q/11}$ (Gα)-mediated activation of phospholipase C $\beta_{1/4}$ ($PLC\beta_{1/4}$), inositol trisphosphate ($InsP_3$), diacylglycerole (DAG), Ca^{2+}, and protein kinase C (PKC). The role of $PLC\beta_1$ and $PLC\beta_4$ in thetagenesis has been validated in knock-out studies using $PLC\beta1^{-/-}$ and $PLC\beta4^{-/-}$ mice exhibiting a complete loss or significant attenuation of theta oscillation[12,13,14]. Additional M_1, M_3, and M_5 downstream targets (channels/currents) of the muscarinic signaling cascade include various conductances, such as M-type K^+ channel (K_M) via voltage-dependent K^+ channel (K_v7); slow after hyperpolarization K^+ channel (Ks_{AHP}); leak K^+ channel (K_{leak}), probably via TWIK-related acid-sensitive K^+ channel (TASK1/3); cation current (I_{CAT}), probably via Na^+ leak channel (NALCN); and I_h via hyperpolarization and cyclic nucleotide gated channels (HCN). In addition, M_2/M_4 acetylcholine receptors (AChRs) were reported to interfere with inward rectifier K^+ channel 3.1 ($K_{ir}3.1$) and inward rectifier K^+ channel 3.2 ($K_{ir}3.2$)[15].

Currently, commercially-available analytical software allows for fast FFT-based frequency analysis, *e.g.,* analysis of power (P, mV^2) or power spectrum density (PSD, mV^2/Hz). Power or power spectrum density (PSD) analysis of the theta frequency range only gives a global overview of its activity. However, in order to get a detailed insight into cognitive and behavior-related theta activity, the analysis of highly-organized theta oscillations is mandatory. The assessment of highly-organized theta oscillations is of central importance in the field of neurodegenerative

and neuropsychiatric diseases. Most experimental disease studies are carried out in transgenic mouse models using highly-sophisticated neurosurgical approaches to record epidural surface and deep intracerebral EEGs. These techniques include both tether systems[16] and radiotelemetric setups[17,18]. Theta oscillations can be recorded as spontaneous and behavior-related theta oscillations under long-term recording conditions. Additionally, theta oscillations can be recorded following pharmacological induction but also following the exposure of animals to behavioral or cognitive tasks or to sensory stimuli, such as tail pinching.

Early approaches to characterize theta oscillations were described by Csicsvari *et al.*[19]. The authors designed a semi-automated tool for short-term theta analysis (15 - 50 min) that is not suitable for long-time EEG recordings. Our method, described here, allows for the analysis of long-term EEG recording > 48 h[20]. Csicsvari *et al.*[10] also referred to the theta-delta ratio, but no threshold for the determination of highly-organized theta oscillations is provided. The delta and theta range definitions match our frequency range definitions. As it is not explicitly mentioned, we presume that an FFT-based method is used by Csicsvari *et al.* to calculate the power of the theta-delta frequency bands. This again clearly differs from our method, since we calculate wavelet-based amplitudes on a large number of frequency scales (frequency steps Δ(f) = 0.05 Hz), resulting in much higher precision. The duration of the individually-analyzed EEG epoch is similar to our definition.

Klausberger *et al.*[21] also make use of theta-delta ratios for the analysis of long-term EEG recordings. However, there are three major differences compared to our approach: i) the EEG epoch duration is much longer, *i.e.,* at least 6 s; ii) the theta-delta ratio is set to 4, which is much higher than our threshold, and is related to different frequency range definitions; and iii) the power definition is likely to be based on an FFT approach, which lacks high precision, particularly for very short time windows (2 s, *i.e.,* 5 cycles for oscillations with a frequency of 2.5 Hz). In such cases, a wavelet-based procedure is more recommendable. A study by Caplan *et al.*[22] solely calculated theta power while ignoring the theta-delta power ratio. Thus, the Caplan approach[22] cannot differentiate between cognitive theta-rich processes accompanied by a high or low delta.

In the following protocol, we will present our analytical wavelet-based approach to reliably analyze highly-organized theta oscillations in hippocampal EEG recordings from mice. Since this procedure works automatically, it can be applied to large data sets and long-term EEG measurements.

Protocol

All animal experimentation was performed according to the guidelines of the local and institutional Council on Animal Care (University of Bonn, BfArM, LANUV, Germany). In addition, all animal experimentation was carried out in accordance with superior legislation, *e.g.,* the European Communities Council Directive of 24 November 1986 (86/609/EEC), or individual regional or national legislation. Specific effort was made to minimize the number of animals used, as well as their suffering.

1. Animal Housing and EEG Recording Conditions

1. House mice in filter-top cages or use individually-ventilated cages.
2. Transfer mice from the animal facility to ventilated cabinets in special lab rooms that are appropriate for implanted animals and telemetric recordings.
3. Perform all animal experimentation, including EEG electrode implantation and the subsequent recordings, under standardized conditions (22 °C temperature, 12 h/12 h light-dark cycle, 50-60% relative humidity, noise attenuation, *etc.*)[18].
4. Prior to radiofrequency transmitter implantation, house animals in groups of 3 - 4 in clear type II polycarbonate cages, with food and water *ad libitum*. Do not isolate individual mice, as this can cause stress and interfere with subsequent experimentation and results.
5. Do not use open housing conditions, but use ventilated cabinets instead during experimentation and recording.

2. Radiotelemetric EEG Electrode Implantation and EEG Recordings

1. **Anesthetize the mice using injection narcotics, *e.g.,* ketaminehydrochloride/xylazinehydrochloride (100/10 mg/kg, intraperitoneally, i.p.) or inhalation narcotics, *e.g.,* isoflurane[17,18].**
    1. For isoflurane narcosis, position the mouse into an induction chamber with 4-5% isoflurane and 0.8-1% oxygen or carbogen (5% CO_2 and 95% O_2).
    2. Place a silicon facemask on the nose/mouth of the animal to control the desired depth of anesthesia and avoid experimenter exposure to isoflurane using a scavenging system.
    3. Use injectable anesthetics, *e.g.,* esketaminhydrochloride (100 mg/kg, i.p.) and xylazinehydrochloride (10 mg/kg, i.p.), if inhalation anesthesia is not available.
    4. Monitor the depth of anesthesia by checking the tail pinch reflex, foot pinch reflex, and respiration rate. Note that artificial respiration *via* tracheal intubation is not necessary in mice.

2. **Implant the radiofrequency transmitter into a subcutaneous pouch on the back of the animal.**
    1. Remove the body hair from the scalp and pretreat the shaved scalp with two disinfectants, *i.e.,* 70% ethanol and an iodine-based scrub.
    2. Using a scalpel, make a midline incision on the scalp from the forehead to the nucheal region.
    3. Starting from the nuchal incision, prepare a subcutaneous pouch on one side of the back of the animal by performing a blunt dissection using surgical scissors or a surgical probe.
    4. Insert the transmitter into the subcutaneous pouch and deposit the excess length of the flexible transmitter leads into the pouch as well. Pay special attention to preventing contamination of the surgical site and transmitter implant. Properly isolate sterile from non-sterile areas using drapes.

3. Place the experimental animal on the stereotaxic frame, *e.g.,* a computerized 3D stereotaxic device. Fix the skull using a nose clamp and ear bars.

4. Pretreat the skull with 0.3% H_2O_2 to remove further tissue from the skull and to illuminate the cranial sutures and craniometrics landmarks, bregma and lambda.
5. Drill holes at the coordinates of choice (see step 2.6) using a high-speed neurosurgical drill in a pressure-free mode at maximum velocity.
   NOTE: Pressure-free drilling avoids the sudden breakthrough of the drill head and damage to the cortex. For a craniotomy, a neurosurgical high-speed drill is recommended. Choose standard drill-head diameters of 0.3 - 0.5 mm, depending on the electrode diameter.
6. Carefully select the electrode type, considering the impedance, diameter, coating, etc.
   NOTE: Parylene-coated tungsten or stainless steel electrodes are the most common. The electrode types should be chosen according to experimental requirements. As a preemptive maneuver, sterilize electrode tips prior to implantation using 70 % ethanol. Note that the electrode coating does not allow for heat sterilization.
7. For intrahippocampal CA1 EEG recordings, drill a hole stereotaxically at the following coordinates: bregma, -2 mm; mediolateral, 1.5 mm (right hemisphere); dorsoventral, 1.3 mm (target region: cornu ammonis (CA1) pyramidal layer). For the reference electrode, drill a hole above the cerebellar cortex at the following stereotaxic coordinates: bregma, -6.2 mm, mediolateral, 0 mm; dorsoventral, 0 mm.
   NOTE: The cerebellar electrode serves as a pseudoreference electrode, as the cerebellum is a rather silent brain region. The stereotaxic coordinates were derived from a standard mouse brain atlas.
8. Prior to the insertion of the electrodes, shorten them to the required length. Mechanically clip the extracranial part of the electrode to the stainless steel helix of the transmitter.
   NOTE: Soldering should be avoided, as this can introduce substantial noise in the system.
9. Attach the electrode to the vertical arm of the stereotaxic device and insert the electrode according to the aforementioned stereotaxic coordinates.
10. Fix the electrodes using glass ionomer cement and wait until the cement has fully hardened.
11. Close the scalp using over-and-over sutures with non-absorbable 5-0 or 6-0 suture material.
12. For postoperative pain management, administer carprofen (5 mg/kg, subcutaneously, s.c.) once a day for 4 consecutive days post-implantation. Note that carprofen should be injected prior to the initial incision (step 2.2.2).
13. Allow the animals to recover for 10 - 14 days post-implantation before the recordings and/or injection experiments are started.

3. Spontaneous Recordings of Theta Oscillations and Pharmacological Induction

1. Activate the radiofrequency transmitter using the magnetic switch. Place the animal with its home cage on the receiver plate. Perform long-term hippocampal EEG recordings for at least 24-48 h.
   NOTE: The analysis of EEG amplitude and EEG frequency characteristics of long-term recordings provides detailed insight into the circadian dependency of theta oscillations and their association with specific behavioral and cognitive conditions/tasks. Always combine EEG recordings with video monitoring of the experimental animals.
2. For pharmacological induction of theta oscillations, administer a single dose of urethane (800 mg/kg i.p.) or a single dose of a muscarinic receptor agonists, e.g. pilocarpine (10 mg/kg i.p.), arecoline (0.3 mg/kg i.p.) or oxotremorine (0.03 mg/kg i.p.). Pretreat mice with N-methylscopolamine (0.5 mg/kg i.p.) to avoid peripheral muscarinic reactions. Freshly dissolve all drugs in 0.9% NaCl or Ringer solution.
   NOTE: Higher dosages of muscarinic receptor agonists might result in seizure induction in experimental animals. Also consider that the dosages given here represent landmarks that require prior dose-effect studies in the mouse line under investigation. Note that urethane is a mutagen and carcinogen that requires appropriate precautions in storage and handling.
3. Inject atropine (50 mg/kg, i.p.) to differentiate atropine-sensitive type II from atropine-insensitive type I theta oscillations.
   NOTE: The atropine dosage is again species- and strain-dependent and requires prior dose-effect evaluation. The optimal time point of atropine injection depends on the pharmacodynamics of muscarinic receptor agonists. For identification of type II theta, atropine injection is recommended 1 h after urethane administration.
4. Try to avoid the subsequent application of several drugs, as systemic drug administration alters global transcriptional and translational patterns, which influence subsequent EEG recordings. Note that short-lasting theta oscillations can also be induced by sensory stimuli, such as tail- or paw-pinching.
5. Extract/export representative EEG data sets of the pre-phase (baseline) and the post-injection phase from the total EEG recording as ASCI or TXT files, considering the pharmacokinetics of the drugs applied and the demands of the individual study protocol.

4. Validation of EEG Electrode Placement

1. Euthanize animals by placing them in an incubation chamber and introduce 100% carbon dioxide. Use a fill rate of 10-30% of the chamber volume per min with carbon dioxide added to the existing air in the incubation chamber; this will result in rapid unconsciousness with minimal stress to the animals.
2. Remove the mouse from the chamber once respiratory arrest occurs and a faded eye color persists for 2-3 min.
3. Cut the stainless steel electrodes and explant the radiofrequency transmitter. Decapitate the mouse using scissors or a guillotine and remove the brain from the neurocranium by gentle manipulation with surgical scissors and forceps.
4. Fix the brains in 4% paraformaldehyde in phosphate buffer saline (PBS) (pH 7.4) overnight. For cryoprotection, transfer the brains to 30% glucose and store them at 4 °C until further processing.
   NOTE: Paraformaldehyde is considered hazardous by the 2012 OSHA Hazard Communication Standard (29 CFR 1910.1200). Take the necessary precautions: use personal protective equipment, ensure appropriate ventilation, and avoid dust formation. In addition, remove sources of ignition and take precautionary measures against static discharges. Paraformaldehyde should not be released into the environment.
5. Mount the extracted brain on the tissue holder of a cryostat using an adhesive and cut the brains into 40 - 75 µm coronal slices. Mount the slices onto glass slides and stain them with Nissl blue using standard histological procedure; this procedure will visualize the branch channel that reflects the previous electrode position. Note that it is also possible to cut coronal slices from the native brain using a vibroslicer
6. Incorporate only those animals that meet correct EEG electrode placement criteria; for the CA1 region, the tip of the deep electrode should be localized inside the CA1 pyramidal layer.

5. Data Acquisition

1. Record CA1 intrahippocampal EEGs with an appropriate sampling rate with no a priori filter cut-off.
   NOTE: The sampling rate, which is transmitter-specific, determines the upper frequency limit of the EEG analysis.
2. Process the recorded data with an analysis software. Program time-frequency analyses and calculations with custom-made procedures for the adequate control of analysis methods (**Figure 5**)[20].
3. Cut the recorded EEG into sections with a length of 1 h each. Use fast computer processors, since computation time is high. Additionally, make use of software that can parallelize computing on multiple kernels[20].

6. EEG Data Analysis

1. Analyze data segments using a complex Morlet wavelet to calculate both the frequency and the amplitude of oscillations.
   NOTE: This wavelet (*e.g.,* $\Psi(x)=(\pi b)^{(-1/2)} \exp(2i\pi cx) \exp(-x^2/b)$, where b is the bandwidth parameter, c the center frequency, and i the imaginary unit) has often been applied in literature to study EEG data, as it guarantees optimal resolution in both frequency and time[23,24].
2. Use a bandwidth parameter and center frequency setting that particularly weights the frequency resolution to distinguish the frequency differences on the 0.1-Hz level while still not neglecting a sufficient time resolution.
   NOTE: Neuronal processes in the gamma band are short-lasting[25], and this can also hold true for theta rhythms. Thus, the analytical approach must consider adequate temporal resolution.
3. Analyze the EEG data in the frequency range of 0.2 - 12 Hz, with a step-size of 0.1 Hz, thus including the typical delta, theta, and alpha frequency ranges.
4. Set up an automated, complex analytical tool for the elaboration of the theta frequency architecture, which can replace a standard visual inspection of theta oscillations; this procedure is called the theta detection method (TDM).
5. Compute the quotient of the maximum amplitude in the theta frequency range (3.5-8.5 Hz) and the maximum amplitude in the upper delta frequency range (2-3.4 Hz) for time windows of 2.5 s each.
   NOTE: The value of this quotient serves as a measure to decide if a theta oscillation occurred. The definition of the theta frequency range can vary depending on the functional state and neuroanatomical circuitry/system to be analyzed.
6. Classify a segment as a "theta oscillatory epoch," if the computed ratio during this segment is above 1.5.
   NOTE: This guarantees that the maximum theta amplitude is at least 50% higher than the amplitude in the upper delta band during the related 2.5-s EEG segment. Note that the ratio might need adaptation depending on the line and/or species used. An interval of 2.5 s represents a minimal duration for a theta oscillation, prevents false-positive detections of certain noisy epochs, and lies within the range definitions of other publications[19,26]. The upper delta frequency range serves as a control frequency band because physiologically-relevant delta activity appears during non-theta epochs, for example, during slow-wave sleep, which is highly dampened during theta activity.
7. Repeat this procedure for every 1 h section; therefore, every section consists of 1,440 EEG segments with lengths of 2.5 s each.
8. Statistically evaluate the data of the identified theta oscillation epochs.
9. Compute the statistics of the total duration times of detected theta epochs; distinct or predefined groups; cycles, such as light/dark; and others parameters.
   NOTE: Statistics may include t-test, ANOVA, or MANOVA, depending on the variable, the number of groups, the conditions, *etc.*
10. Calculate the statistics of the amplitude of the detected theta epochs, but only in the theta frequency range (3.5 - 8.5 Hz).
11. Evaluate the statistics of the frequency of the detected theta epochs, but only in the theta frequency range (3.5 - 8.5 Hz).
    NOTE: The theta frequency of a theta epoch is defined as the frequency belonging to the maximum theta amplitude of a theta epoch.

Representative Results

Theta activity can be recorded in a wide range of central nervous system (CNS) regions. Here, we present an analysis of theta oscillations from the murine hippocampus. Such oscillations can occur during different behavioral and cognitive states. It is highly recommended to analyze theta oscillations under both spontaneous long-term, task-related short-term, and pharmacologically-induced conditions.
Figure 1 illustrates a representative intrahippocampal CA1 recording under control conditions. If the animal is not in a spontaneous "theta state," the intrahippocampal EEG is often characterized by large-irregular-amplitude (LIA) activity. Administration of muscarinic receptor agonists (*e.g.,* arecoline, pilocarpine, or urethane) results in highly-organized theta oscillations that can be blocked by atropine (50 mg/kg, i.p., **Figure 1**).

In order to quantify highly-organized theta oscillations with the appropriate time resolution, the theta detection tool was used to classify 2.5 s EEG epochs as either theta-negative or theta-positive (**Figure 2**). Based on this classification, it is possible to quantify the total duration of theta oscillations under spontaneous conditions or specific behavioral and cognitive tasks.

In order to analyze a 30-min EEG segment (as for pharmacological urethane/atropine theta dissection), we first perform a time-frequency analysis for a frequency range of 0.2-12 Hz, which displays the amplitude (mV) in a color-coded fashion (**Figure 3 A**). As becomes obvious in **Figure 3 A**, high-amplitude theta activity, which is confirmed by a visual inspection of the EEG (white arrows), is accompanied by a low amplitude in the delta frequency range. Then, the maximum amplitudes of the theta (3.5-8.5 Hz) and delta (2-3.4 Hz) frequency ranges are plotted (**Figure 3 B**). Systematic correlation studies revealed that the ratio of maximum theta amplitude to maximum delta amplitude exceeding 1.5, indicating highly-organized theta oscillations (**Figure 3 C**).
Figure 4 demonstrates how urethane can induce hippocampal theta oscillations (white circles in **Figure 4 II**). Urethane is a multi-target drug that can trigger type II theta due its agonistic action on muscarinic receptors. Following an atropine injection (**Figure 4 III**), these type II theta oscillations (atropine-sensitive theta oscillations) are abolished. It is important to consider that the muscarinic receptor agonists, in addition to atropine, have individual pharmacokinetic properties that affect the time characteristics of theta occurrence and theta blockade. It should be noted that atropine-insensitive type I theta remains unaffected by muscarinic receptor antagonists.

A summary of the whole theta detection and quantification tool is depicted in **Figure 5**. It results in the calculation of the amplitude, frequency, and sum/mean theta duration. In contrast to previously-described techniques, it makes use of a wavelet-based approach with high precision. The analytical tool described here has several fields of application. Theta oscillations are generated in the septohippocampal system and are often impaired by neurodegenerative processes, *e.g.,* in Alzheimer's disease. Numerous mouse models of Alzheimer's disease have been described that vary in homology, isomorphism, and predictability. Some of these models were reported to exhibit a reduction in theta activity, whereas others were shown to display an increase in theta activity, the reason for which remains to be determined. We successfully applied the theta detection tool described here to characterize altered theta oscillatory architecture in the 5XFAD model of Alzheimer's disease[8]. However, it might also be applied in epilepsy research and neuropsychiatric diseases.

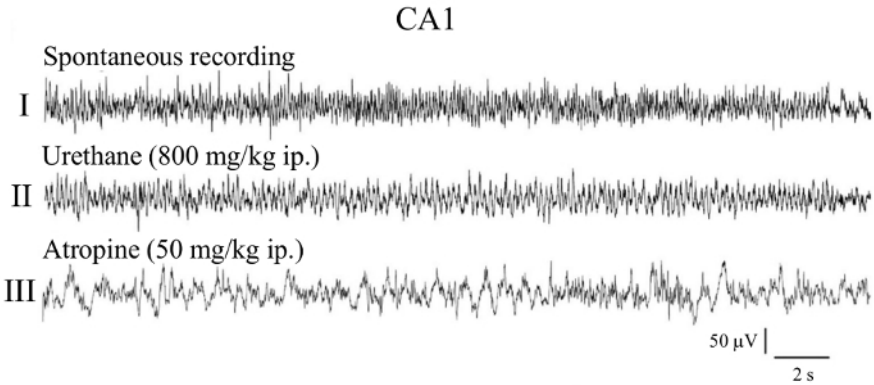

Figure 1: Theta Oscillations in C57Bl/6 Mice. Radiotelemetric intrahippocampal CA1 recording under spontaneous conditions (I) and following urethane injection (800 mg/kg, i.p., II). Following urethane injection, highly-organized theta oscillations become visible, which can be blocked by atropine (50 mg/kg, i.p.). This figure has been modified from reference[20], with permission. Please click here to view a larger version of this figure.

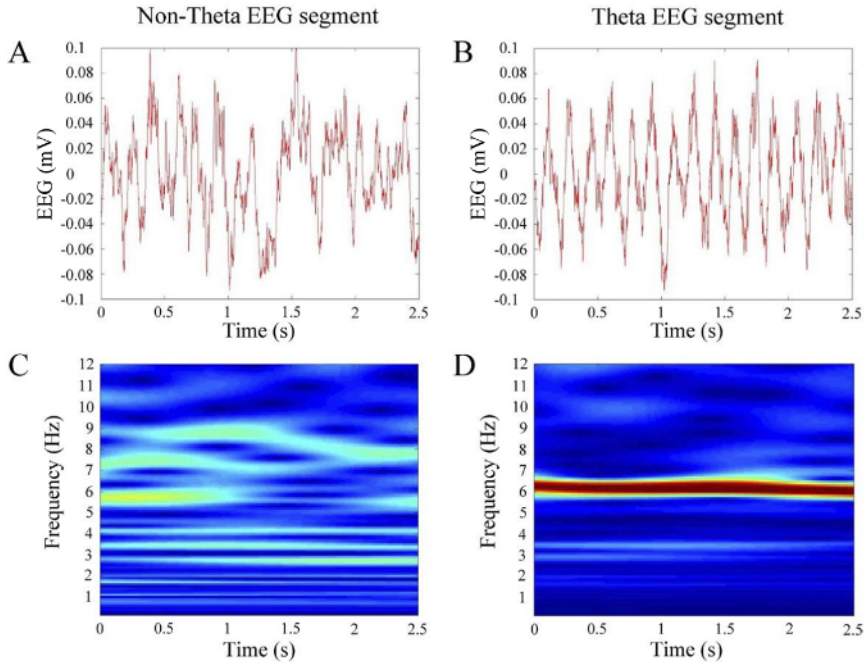

Figure 2: A Wavelet-based Analysis of a Deep CA1 EEG Recording from a C57Bl/6 Mouse. (**A** and **B**) Two 2.5-s EEG epochs are depicted, visually classified as non-theta and theta segments, respectively. (**C** and **D**) Time-frequency analysis of the CA1 EEG segments displayed in **A** and **B** in the range of 0.2-12 Hz, with the amplitude being color-coded. The time-frequency analysis in **C** exhibits irregular, fluctuating theta architecture regarding frequencies and time, whereas a segment with highly synchronized theta oscillations is characterized by a regular, non-fluctuating high amplitude theta of a nearly constant frequency of 6 Hz. The ratio of maximum theta to maximum delta amplitude is 1.25 in **C** and 4.67 in **D**, clearly classifying **B** as a theta oscillation EEG segment. This figure was reprinted from Reference 20, with permission. Please click here to view a larger version of this figure.

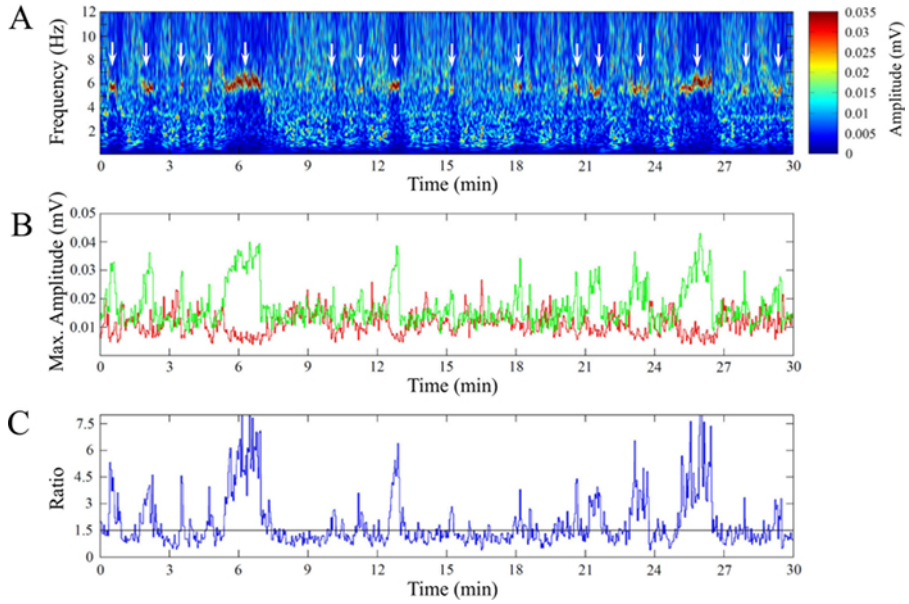

Figure 3: A Wavelet-based Theta Detection Tool. (**A**) Time-frequency analysis of a 30 min EEG segment (not shown) that has been recorded following urethane administration. The complex Morlet wavelet-based analysis was performed in the range of 0.2-12 Hz, with the amplitude (mV) being color-coded. (**B**) This image displays the maximum amplitude of the theta frequency band (3.5-8.5 Hz, green) and the upper delta band (2-3.4 Hz, red) for the 30-min EEG segment. (**C**) This figure illustrates the ratio of the maximum theta amplitude (green in **B**) and the maximum delta amplitude (red in **B**). Note that highly-synchronized theta oscillations correlate with suprathreshold ratios in C. This figure was reprinted from Reference 20, with permission. Please click here to view a larger version of this figure.

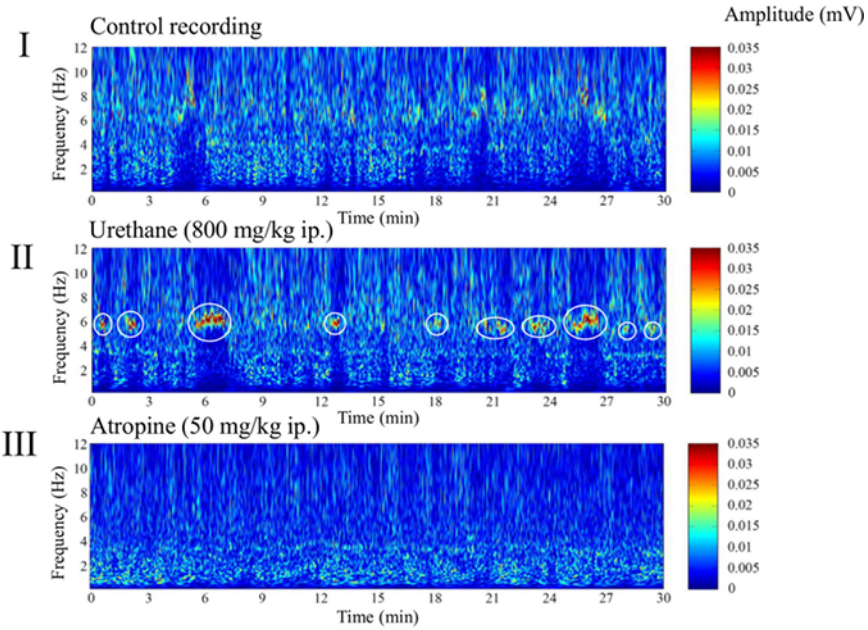

Figure 4: Wavelet-based Analysis of Pharmacologically-induced, Highly-organized Theta Oscillations. Representative 30-min EEG segments (not shown) are analyzed in the frequency range of 0-12 Hz with the amplitude (mV) being color-coded. A urethane injection at 800 mg/kg, i.p., resulted in the fragmented occurrence of highly-organized theta oscillations, with a predominant frequency of about 6 Hz (white circles). Following an atropine injection at 50 mg/kg, i.p., these theta oscillations are abolished. This figure was reprinted from Reference 20, with permission. Please click here to view a larger version of this figure.

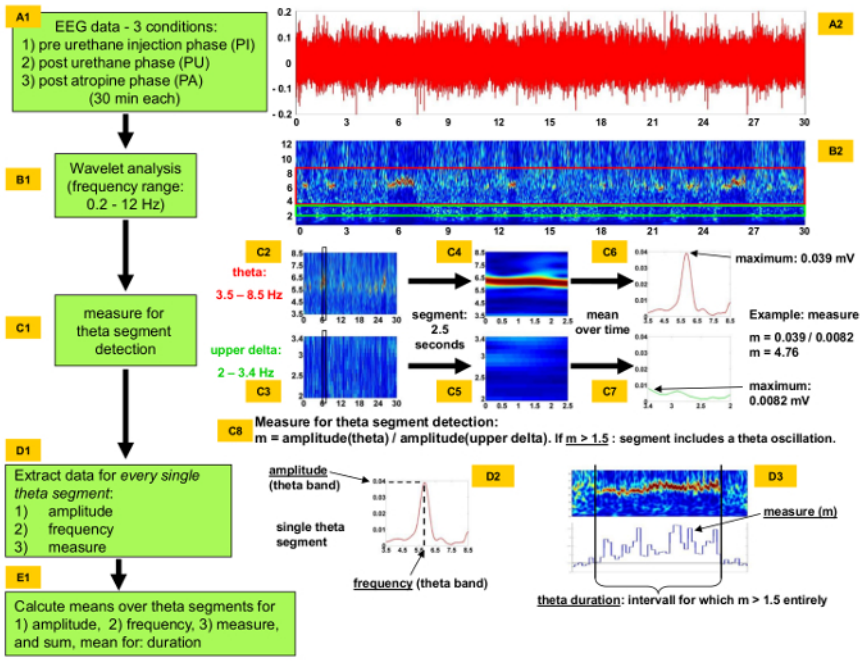

Figure 5: Flow Diagram Illustrating the Quantification of Highly-organized Theta Oscillations Recorded from the Murine CA1. Type II theta oscillations can be analyzed using a control recording (phase), a post-injection (*e.g.,* urethane, arecoline, or pilocarpine) phase, and a post-atropine phase (**A1**). 30 min EEG segments (**A2**) from each phase are time-frequency analyzed in the range from 0.2-12 Hz using a wavelet-based approach (**B1** and **B2**). Next, theta segment detection is initiated (**C1**), giving a closer look at the time-frequency characteristics of theta range (3.5-8.5 Hz, **C2**) and the upper delta range (2-3.4 Hz, **C3**) for EEG epochs that are 2.5 s each (**C4** and **C5**). Subsequently, the amplitude is analyzed over the theta and delta frequency range depicting the maximum values (**C6** and **C7**). If the maximum amplitude of theta/delta exceeds 1.5, the 2.5 s EEG segment is classified as an epoch of highly-organized theta oscillation (**C8**), with a defined amplitude and frequency (**D1-D3**). This theta detection tool allows for the quantification of theta oscillation architecture (**E1**). Please click here to view a larger version of this figure.

Discussion

Theta activity is of central relevance in systemic neurophysiology. It can be observed in various brain regions, particularly in the hippocampus, where it is related to specific behavioral and cognitive states. In addition, hippocampal theta can be pharmacologically differentiated into atropine-sensitive type II and atropine-insensitive type I theta. Type I is thought to be related to locomotion, such as walking or running[27,28,29,30,31], whereas type II can be observed during the alert-immobility state[27,28,29,30]. Alert-immobility states can be induced by infrequent and random tone or tactile stimuli, for example[32]. Type II theta is also related to passive whole-body rotation[14]. During paradoxical sleep, both atropine-sensitive and atropine-resistant theta rhythms are present[33]. The resting-immobility state is characterized by large irregular activity (LIA)[27].

In general, theta oscillations can be recorded under spontaneous conditions, but also following pharmacological induction (*e.g., via* the application of muscarinic receptor agonists, such as urethane, pilocarpine, arecoline, oxotremorine, *etc.*). Note that, pharmacodynamically, urethane is a multi-target drug that can enhance type II theta but also inhibit type I theta. In contrast, pilocarpine, arecoline, and oxotremorine selectively induce type II theta. Depending on the pharmacokinetics of the muscarinic agonists used, it takes a variable amount of time until theta oscillations occur. Type II can be blocked effectively by atropine. Critically, the dosages of muscarinic agonists and antagonists to induce and block type II theta oscillations are species- and strain-dependent. Thus, it is absolutely essential to perform dose-effect studies to unravel the optimal dose for the induction of theta oscillations and for their blockage for a specific scientific question. Short-lasting theta oscillations can also be induced by sensory stimuli, such as tail- or paw-pinching.

There are different approaches to characterize theta activity in general. FFT-based approaches, resulting in continuous or discontinuous (frequency band-related) power spectrum density (PSD) analysis/plots or in a power analysis for individual frequency bands, are standard approaches that provide valuable information on frequency characteristics.

However, to achieve a more complex insight into theta architecture, additional approaches seem to be necessary. In particular, one might be interested in the different organizational states of theta and their frequencies, which cannot be assessed directly and accurately by the aforementioned procedures. In contrast, the novel analytical technique presented here is wavelet-based and capable of evaluating highly-organized, short-term theta oscillations. They do not correspond to standard theta power, which also considers paroxysmal, discontinuous theta activity. The focus is to elicit specific time-frequency characteristics in the EEG data that are typical for theta epochs. Thus, the new method prevents false-positive classifications of theta epochs. The automated procedure guarantees the evaluation of long-lasting EEG data sets and therefore includes reliable statistical comparisons of physiological cycles (light/dark cycle or circadian rhythmicity) during long-term studies.

This protocol is of special importance in the analysis of EEG data obtained from animal models of neurodegenerative diseases, particularly in the characterization of highly-organized theta architecture in the septohippocampal and other neural systems. Complex and high-precision theta analysis might help to determine EEG fingerprints that can serve as EEG biomarkers in the future.

Disclosures

The authors have nothing to disclose.

Acknowledgements

The authors would like to thank Dr. Christina Ginkel (German Center for Neurodegenerative Diseases, DZNE) and Dr. Robert Stark (DZNE) for their assistance with animal breeding and animal healthcare. This work was financially supported by the Federal Institute for Drugs and Medical Devices (Bundesinstitut für Arzneimittel und Medizinprodukte, BfArM), Bonn, Germany.

References

1. Vanderwolf, C. H. Hippocampal electrical activity and voluntary movement in the rat. *Electroencephalogr Clin Neurophysiol.* **26**, 407-418 (1969).
2. Kahana, M. J., Seelig, D., & Madsen, J. R. Theta returns. *Curr Opin Neurobiol.* **11**, 739-744 (2001).
3. Varga, V. *et al.* The presence of pacemaker HCN channels identifies theta rhythmic GABAergic neurons in the medial septum. *J Physiol.* **586**, 3893-3915 (2008).
4. Takano, Y., & Hanada, Y. The driving system for hippocampal theta in the brainstem: an examination by single neuron recording in urethane-anesthetized rats. *Neurosci Lett.* **455**, 65-69 (2009).
5. Goutagny, R., Manseau, F., Jackson, J., Danik, M., & Williams, S. In vitro activation of the medial septum-diagonal band complex generates atropine-sensitive and atropine-resistant hippocampal theta rhythm: an investigation using a complete septohippocampal preparation. *Hippocampus.* **18**, 531-535 (2008).
6. Manseau, F., Goutagny, R., Danik, M., & Williams, S. The hippocamposeptal pathway generates rhythmic firing of GABAergic neurons in the medial septum and diagonal bands: an investigation using a complete septohippocampal preparation in vitro. *J Neurosci.* **28**, 4096-4107 (2008).
7. Hangya, B., Borhegyi, Z., Szilagyi, N., Freund, T. F., & Varga, V. GABAergic neurons of the medial septum lead the hippocampal network during theta activity. *J Neurosci.* **29**, 8094-8102 (2009).
8. Siwek, M. E. *et al.* Altered theta oscillations and aberrant cortical excitatory activity in the 5XFAD model of Alzheimer's disease. *Neural Plast.* **2015**, 781731 (2015).
9. Buzsaki, G. Theta oscillations in the hippocampus. *Neuron.* **33**, 325-340 (2002).
10. Buzsaki, G. *et al.* Hippocampal network patterns of activity in the mouse. *Neuroscience.* **116**, 201-211 (2003).
11. Buzsaki, G., & Moser, E. I. Memory, navigation and theta rhythm in the hippocampal-entorhinal system. *Nat Neurosci.* **16**, 130-138 (2013).
12. Shin, J. Theta rhythm heterogeneity in humans. *Clin Neurophysiol.* **121**, 456-457 (2010).
13. Shin, J. *et al.* Phospholipase C beta 4 in the medial septum controls cholinergic theta oscillations and anxiety behaviors. *J Neurosci.* **29**, 15375-15385 (2009).
14. Shin, J., Kim, D., Bianchi, R., Wong, R. K., & Shin, H. S. Genetic dissection of theta rhythm heterogeneity in mice. *Proc Natl Acad Sci U S A.* **102**, 18165-18170 (2005).
15. Brown, D. A., & Adams, P. R. Muscarinic suppression of a novel voltage-sensitive K^+ current in a vertebrate neurone. *Nature.* **283**, 673-676 (1980).
16. Senkov, O., Mironov, A., & Dityatev, A. A novel versatile hybrid infusion-multielectrode recording (HIME) system for acute drug delivery and multisite acquisition of neuronal activity in freely moving mice. *Front Neurosci.* **9**, 425 (2015).
17. Lundt, A. *et al.* EEG Radiotelemetry in Small Laboratory Rodents: A Powerful State-of-the Art Approach in Neuropsychiatric, Neurodegenerative, and Epilepsy Research. *Neural Plast.* **2016**, 8213878 (2016).
18. Papazoglou, A. *et al.* Non-restraining EEG radiotelemetry: epidural and deep intracerebral stereotaxic EEG electrode placement. *J Vis Exp.* (112) (2016).
19. Csicsvari, J., Hirase, H., Czurko, A., & Buzsaki, G. Reliability and state dependence of pyramidal cell-interneuron synapses in the hippocampus: an ensemble approach in the behaving rat. *Neuron.* **21**, 179-189 (1998).
20. Muller, R. *et al.* Atropine-sensitive hippocampal theta oscillations are mediated by $Ca_v2.3$ R-type Ca^{2+} channels. *Neuroscience.* **205**, 125-139 (2012).
21. Klausberger, T. *et al.* Brain-state- and cell-type-specific firing of hippocampal interneurons in vivo. *Nature.* **421**, 844-848 (2003).
22. Caplan, J. B., Madsen, J. R., Raghavachari, S., & Kahana, M. J. Distinct patterns of brain oscillations underlie two basic parameters of human maze learning. *J Neurophysiol.* **86**, 368-380 (2001).
23. Montgomery, S. M., & Buzsaki, G. Gamma oscillations dynamically couple hippocampal CA3 and CA1 regions during memory task performance. *Proc Natl Acad Sci U S A.* **104**, 14495-14500 (2007).
24. Kronland-Martinet, R., Morlet, J., & Grossman, A. Analysis of sound patterns through wavelet transform. *Int J Pattern Recognit Artif Intell.* **1**, 29 (1987).
25. Buzsaki, G., & Wang, X. J. Mechanisms of gamma oscillations. *Annu Rev Neurosci.* **35**, 203-225 (2012).
26. Goutagny, R., Jackson, J., & Williams, S. Self-generated theta oscillations in the hippocampus. *Nat Neurosci.* **12**, 1491-1493 (2009).
27. Bland, B. H. The physiology and pharmacology of hippocampal formation theta rhythms. *Prog Neurobiol.* **26**, 1-54 (1986).
28. Leung, L. S. Generation of theta and gamma rhythms in the hippocampus. *Neurosci Biobehav Rev.* **22**, 275-290 (1998).
29. Shin, J., & Talnov, A. A single trial analysis of hippocampal theta frequency during nonsteady wheel running in rats. *Brain Res.* **897**, 217-221 (2001).

30. Shin, J. A unifying theory on the relationship between spike trains, EEG, and ERP based on the noise shaping/predictive neural coding hypothesis. *Biosystems.* **67**, 245-257 (2002).
31. Kramis, R., Vanderwolf, C. H., & Bland, B. H. Two types of hippocampal rhythmical slow activity in both the rabbit and the rat: relations to behavior and effects of atropine, diethyl ether, urethane, and pentobarbital. *Exp Neurol.* **49**, 58-85 (1975).
32. Lu, B. L., Shin, J., & Ichikawa, M. Massively parallel classification of single-trial EEG signals using a min-max modular neural network. *IEEE Trans Biomed Eng.* **51**, 551-558 (2004).
33. Robinson, T. E., Kramis, R. C., & Vanderwolf, C. H. Two types of cerebral activation during active sleep: relations to behavior. *Brain Res.* **124**, 544-549 (1977).

